Light-Intensity Distributions in Distributed-Feedback Resonators

Jerry Yeung[1] and Markus Pollnau[1]
[1] Advanced Technology Institute, Department of Electrical and Electronic Engineering, University of Surrey, Guildford GU2 7XH, United Kingdom
e-mail: m.pollnau@surrey.ac.uk

ABSTRACT

Based on the circulating-field approach that has been used to calculate the optical properties of Fabry-Pérot resonators, we introduce a simple recursive method to obtain the exact electric-field and intensity distributions in arbitrary multi-resonator structures exhibiting intrinsic propagation losses. Reflectivity, transmissivity, and propagation-loss curves and light-intensity distributions along the resonator axis are calculated for distributed-feedback (DFB) resonators with uniform propagation losses and consequences for DFB lasers are discussed.

Keywords: Bragg gratings, distributed-feedback resonators, intensity distributions, calculation methods.

1. INTRODUCTION

The performance of Bragg gratings and distributed-feedback (DFB) resonators has been modeled by the coupled-mode theory [1,2], which is an approximated formalism that has been extended in various ways to better approximate specific configurations. Alternatively, the characteristic-matrix approach [3,4] provides exact solutions, at the expense of larger computing efforts. Equally exact, but avoiding the matrix formalism, is the impedance method [5]. By use of these theories, frequently reflection and transmission curves of Bragg gratings and DFB resonators without propagation losses have been calculated. In some cases, either propagation losses have been included or light-intensity distributions at the Bragg wavelength have been modeled. For predicting and optimizing the performance of on-chip DFB lasers [6,7] and their ultra-narrow linewidths, however, a deeper understanding of the underlying passive DFB resonator including propagation losses, the laser-active DFB resonator with gain, and the intensity distribution along the resonator axis at the resonance wavelength are required.

In this paper, a recursive method based on the circulating-field approach [8] is introduced to calculate the exact reflection and transmission curves and light-intensity distributions in DFB resonators with propagation losses.

2. EXACT CALCULATION OF GRATINGS AND DFB RESONATORS WITH PROPAGATION LOSS

Each Fabry-Pérot resonator j has an individual length ℓ_j, is homogeneously filled with a medium of individual refractive index $n_{r,j}$, resulting in the speed of light inside the resonator of $c_j = c_0/n_{r,j}$, where c_0 is the speed of light in vacuum, and a round-trip time of $t_{RT,j} = 2\ell_j/c_j$. The accumulated round-trip phase $2\phi_j$ in each resonator at frequency ν is given by

$$2\phi_j(\nu) = 2\pi\nu t_{RT,j} = 2\pi\nu\frac{2\ell_j}{c_j} = 2\pi\nu\frac{2\ell_j}{c_0/n_{r,j}}. \quad (1)$$

The amplitude and intensity reflectivities r_j and R_j and amplitude and intensity transmissions t_j and T_j, respectively, of the mirrors or interfaces $j = 1, \ldots, N+1$ are

$$|r_j|^2 = R_j = 1 - |t_j|^2 = 1 - T_j. \quad (2)$$

If the reflectivities are solely resulting from the interface between media of different refractive index, then the reflectivity r_j and transmissivity t_j of each mirror j are given by the Fresnel equations.

The situation of the simplest multi-resonant structure, a double Fabry-Pérot resonator, is displayed in Figure 1. The relevant refractive indices, resonator lengths, amplitude reflectivities, and electric fields E are indicated.

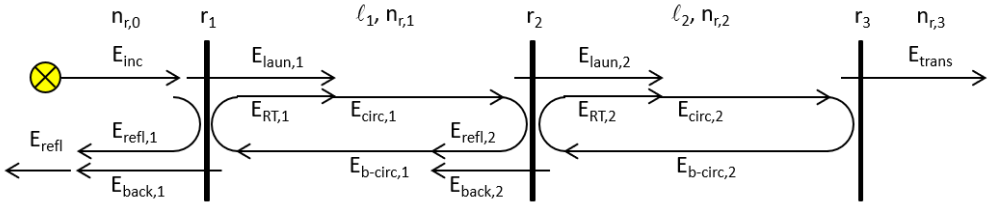

Figure 1. Double Fabry-Pérot resonator with relevant electric fields E; inc: incident; refl: reflected; laun: launched; circ: forward-circulating; b-circ: backward-circulating; RT: round-trip; trans: transmitted.

The circulating-field approach [8] has previously been applied to single Fabry-Pérot resonators [9]. It can straightforwardly be extended to the situation of a multiple Fabry-Pérot-resonator structure. The relationships between the electric fields in the double-Fabry-Pérot resonator of Figure 1 are

$$E_{circ,1} = it_1 E_{inc} + r_1 e^{-i\phi_1} e^{-\alpha_{loss}/2} E_{b-circ,1}, E_{b-circ,1} = r_2 e^{-i\phi_1} e^{-\alpha_{loss}/2} E_{circ,1} + it_2 e^{-i\phi_2} e^{-\alpha_{loss}/2} E_{b-circ,2} \quad (3)$$

$$E_{circ,2} = it_2 e^{-i\phi_1} e^{-\alpha_{loss}/2} E_{circ,1} + r_2 e^{-i\phi_2} e^{-\alpha_{loss}/2} E_{b-circ,2}, E_{b-circ,2} = r_3 e^{-i\phi_2} e^{-\alpha_{loss}/2} E_{circ,2}, \quad (4)$$

where α_{loss} is the intensity-loss coefficient per unit length. These equations can be exploited to describe the electric-field distributions of a structure with *N* consecutive Fabry-Pérot resonators. As long as there is no light launched from the other end of the multi-resonator structure, the electric fields for all resonators are given by

$$\frac{E_{circ,j}}{E_{circ,j-1}} = \frac{it_j e^{-i\phi_{j-1}} e^{-\alpha_{loss}/2}}{1 - r_j r_{j+1} e^{-i2\phi_j} e^{-\alpha_{loss}} - r_j i t_{j+1} e^{-i\phi_j} e^{-i\phi_{j+1}} e^{-\alpha_{loss}} \frac{E_{b-circ,j+1}}{E_{circ,j}}}, \quad (5)$$

$$\frac{E_{b-circ,j}}{E_{circ,j-1}} = \left(r_{j+1} e^{-i\phi_j} e^{-\alpha_{loss}/2} + it_{j+1} e^{-i\phi_{j+1}} e^{-\alpha_{loss}/2} \frac{E_{b-circ,j+1}}{E_{circ,j}} \right) \frac{E_{circ,j}}{E_{circ,j-1}}. \quad (6)$$

By applying these equations recursively, the exact electric-field distribution along the grating can be found.

3. OUTPUT AND LOSS CHARACTERISTICS, INTENSITY DISTRIBUTIONS

In Figure 2, the reflectivity, transmissivity, and loss curves of DFB resonators with the design parameters of Table 1 and four different loss-coefficient values are displayed. In all cases, $R+T+loss=1$. In the large-reflectivity region the reflectivity decreases with increasing losses, whereas the transmissivity remains unaffected. At the resonant wavelength, the reflectivity increases but also the transmissivity decreases significantly with increasing losses, indicating a loss of resonance. At low propagation losses, the highest loss occurs at the Bragg wavelength, but as the propagation losses increase, the highest loss now occur at either end of the stopband.

Table 1: DFB grating parameters

Number of films	4485	Low eff. refractive index	1.6049715
Bragg wavelength	1.5500e-06 m	Grating length	1.0818413 cm
High eff. refractive index	1.6079535	Phase-shift position	0.5409207 cm

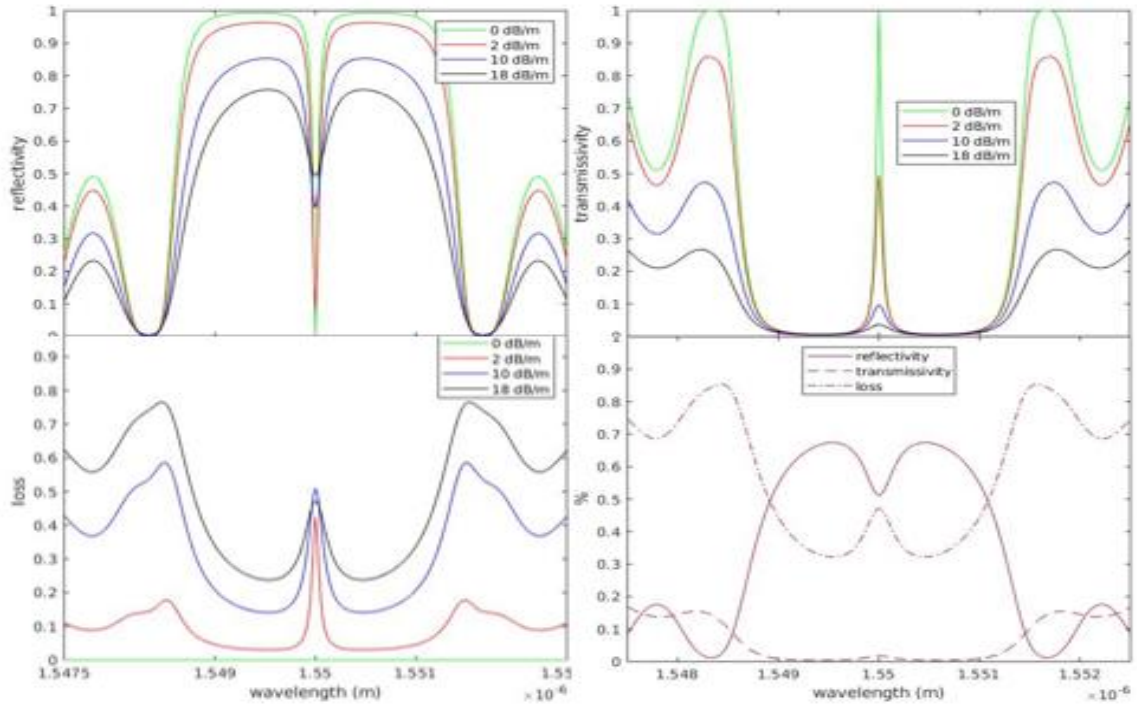

Figure 2. (Top left) Reflectivity, (top right) transmissivity, and (bottom left) loss curves for different propagation losses (legend). (Bottom right) Reflectivity, transmissivity, and loss curves for a propagation loss of α_{loss} = 26 dB/m.

Figure 3 shows the intensity distributions along the grating length for different wavelengths and propagation losses. At the Bragg wavelength, the resonance enhancement decreases significantly with increasing losses. The asymmetry of the distribution is due to light entering the grating from the left side only. As we move further away from the Bragg wavelength, an intensity jump occurs at the phase shift region. The bottom-left figure shows the intensity distribution at the wavelength at which ρ [10] changes from real to imaginary. Beyond, the intensity distribution displays oscillatory behavior, though this effect is less pronounced as propagation losses increase.

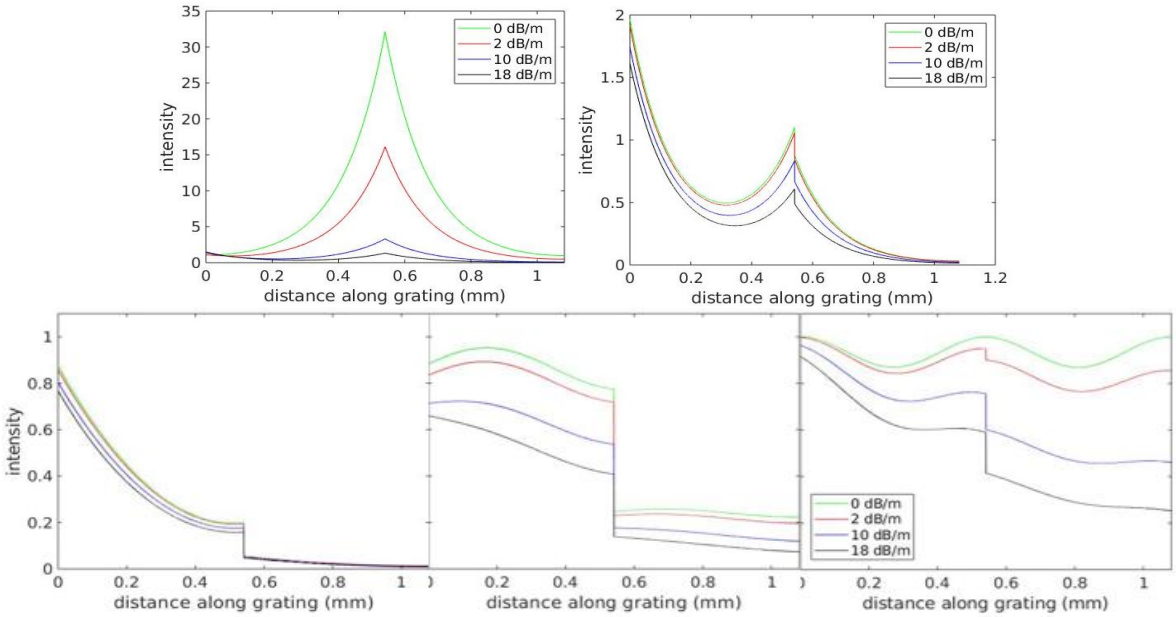

Figure 3. Intensity distribution versus grating position for different wavelengths: (top left) $\lambda = 1.5000\times10^{-6}$ m (= Bragg wavelength), (top right) $\lambda = 1.5498\times10^{-6}$ m, (bottom left) $\lambda = 1.5491\times10^{-6}$ m (= critical wavelength), (bottom middle) $\lambda = 1.5487\times10^{-6}$ m, and (bottom right) $\lambda = 1.5484e\times10^{-6}$ m (= wavelength of first zero reflection), for different propagation losses (legend).

Finally, at wavelengths far away from the Bragg wavelength, full oscillatory behaviour is present without losses, whereas a combination of exponential and oscillatory behaviour is observed when propagation losses are present.

4. CONCLUSIONS

We have presented a simple, straight-forward method, based on the recursive calculation of single Fabry-Pérot resonators, to calculate the exact intensity distributions within a DFB resonator. Uniform propagation losses have been considered. The resulting output and loss curves, as well as the intensity distribution along the resonator axis have been calculated and their behavior studied. These results will help predict the performance of DFB lasers.

ACKNOWLEDGEMENTS

The authors thank Cristine Kores, Nur Ismail, and Edward Bernhardi for helpful discussions and acknowledge funding by the European Research Council (ERC) Advanced Grant “Optical Ultra-Sensor” No. 341206.

REFERENCES

[1] H. Kogelnik, C.V. Shank: Coupled-wave theory of distributed feedback lasers, *J. Appl. Phys.*, vol. 43, pp. 2327-2335, 1972.

[2] A. Yariv: Coupled-mode theory for guided-wave optics, *IEEE J. Quantum Electron.*, vol. QE9, pp. 919-933, 1973.

[3] C.C. Kores, N. Ismail, D. Geskus, M. Dijkstra, E.H. Bernhardi, M. Pollnau: Temperature dependence of the spectral characteristics of distributed-feedback resonators, *Opt. Express*, vol. 26, pp. 4892-4905, 2018.

[4] M. Born, E. Wolf: *Principles of Optics*, Pergamon, 1975, Ch. 1.

[5] N.M. Kondratiev, A.G. Gurkovsky, M.L. Gorodetsky: Thermal noise and coating optimization in multilayer dielectric mirrors, *Phys. Rev. D*, vol. 84, art. 022001, 2011.

[6] E.H. Bernhardi, H.A.G.M. van Wolferen, L. Agazzi, M.R.H. Khan, C.G.H. Roeloffzen, K. Wörhoff, M. Pollnau, R.M. de Ridder: Ultra-narrow-linewidth, single-frequency distributed feedback waveguide laser in Al_2O_3:Er^{3+} on silicon, *Opt. Lett.*, vol. 35, pp. 2394-2396, 2010.

[7] C.T. Santis, S.T. Steger, Y. Vilenchik, A. Vasilyev, A. Yariv: High-coherence semiconductor lasers based on integral high-Q resonators in hybrid Si/III-V platforms, *Proc. Natl. Acad. Sci. USA*, vol. 111, pp. 2879-2884, 2014.

[8] A.E. Siegman: Lasers, University Science Books, Mill Valley, CA, 1986, ch. 11.3, pp. 413-428.

[9] N. Ismail, C.C. Kores, D. Geskus, M. Pollnau, Fabry-Pérot resonator: Spectral line shapes, generic and related Airy distributions, linewidths, finesses, and performance at low or frequency-dependent reflectivity, *Opt. Express*, vol. 24, pp. 16366-16389, 2016.

[10] M. Yamada, K. Sakuda: Analysis of almost-periodic distributed feedback slab waveguides via a fundamental matrix approach, *Appl. Opt.*, vol. 26, pp. 3474-3478, 1987.